POLITECNICO
MILANO 1863

DIPARTIMENTO DI MECCANICA

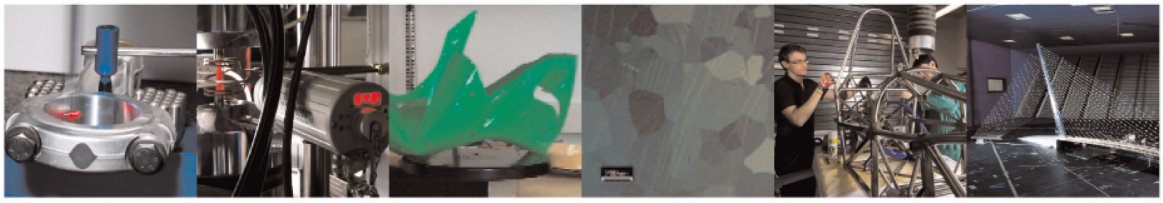

A 3D printed Ti6Al4V alloy uniaxial capacitive accelerometer

Valentina Zega, Luca Martinelli, Riccardo Casati, Emanuele Zappa, Giacomo Langfelder, Alfredo Cigada, and Alberto Corigliano

This is a post-peer-review, pre-copyedit version of an article published in *IEEE Sensors Journal*. The final authenticated version is available online at:
http://dx.doi.org/10.1109/JSEN.2021.3095760

A 3D printed Ti6Al4V alloy uniaxial capacitive accelerometer

Valentina Zega, Luca Martinelli, Riccardo Casati, Emanuele Zappa, Giacomo Langfelder, Alfredo Cigada, and Alberto Corigliano

***Abstract*— 3D-printing techniques are attracting a lot of interest in the sensors community as promising fabrication processes that guarantees customizability at low costs. In this work, the first uniaxial Ti6Al4V alloy accelerometer is designed, fabricated through the Laser Powder Bed Fusion (L-PBF) technique and tested. Experimental tests under accelerations show good agreement with theoretical predictions. With a differential sensitivity of 184fF/g and relative low dimensions (features as low as 500µm), the proposed accelerometer opens the path to a new class of 3D-printed metal sensors with high-performance, customizability and low-cost.**

***Index Terms*—3D-printing technique, uniaxial accelerometer, experimental characterization.**

I. Introduction

MICRO-ELECTRO-MECHANICAL systems (MEMS) dominate the sensors market so far thanks to their low cost and small dimensions [1]. Recently, novel fabrication processes are emerging to satisfy the increasing request of three-dimensionality and customizability at low cost [2]-[3], that are not fully achievable so far with standard MEMS processes based on mostly planar technology and large scale production.

In particular, printing techniques [4] are playing a big role in the sensor field, especially for applications where small dimensions are not important and large scale production is not required [5]-[6]. In [7]-[8], for example, 3D-printing methods are exploited to integrate a mechanical sensor with its flexible electronics. Inkjet-printing has been also recently employed in combination with 3D-printing to fabricate customized sensors [9]-[10]. Inkjet-printing of metal structures is widely employed in electrochemical sensor applications for the low waste and affordable costs [11]. As another example, a smart combination of 3D-printing and wet-metallization has been recently proposed by co-Authors for the realization of capacitive uniaxial and three-axial accelerometers [12]-[13] and Coriolis flow-meters [14].

In this framework, 3D-printed metal sensors emerge as a valid alternative since, while keeping three-dimensionality and customizability at low cost of polymer-based sensors, show intrinsic electrical conductivity that makes the fabrication process smoother and promising for a lot of applications. Moreover, metal sensors can in principle overcome the main limitations of polymer based sensors in harsh environments, e.g. high temperature.

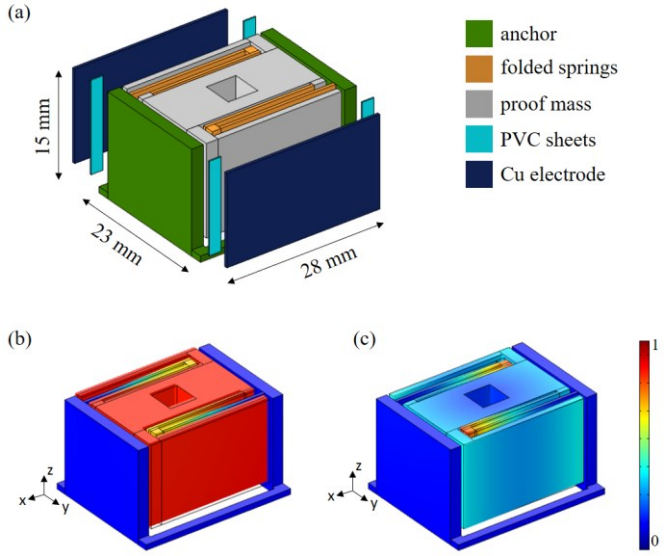

Fig. 1. (a) Schematic view of the capacitive uniaxial accelerometer. (b) First *y*-axis translational mode (f = 200 Hz). (c) First spurious mode of the accelerometer: *z*-axis rotation of the proof mass (f = 750 Hz). The contour of the normalized displacement field is shown in color.

Among other techniques, Laser Powder Bed Fusion (L-PBF) is the best candidate for the fabrication of such prototypes [15] owing to achievable mechanical properties [16]-[18] and good resolution [19].

To the Authors' best knowledge, there are no examples of 3D-printed metal capacitive sensors available so far. In [20], sensors are embedded in an L-PBF part for temperature monitoring, whereas in [21] sensors are used for in-process sensing, but none of these works present the fabrication of sensors through the PBF processes.

In this work, we present the design, fabrication and

Manuscript received …; revised…; accepted ….. Date of publication ….; date of current version ….. This work was carried out in the framework of the inter-departmental laboratory MEMS&3D of Politecnico di Milano.

V. Zega, L. Martinelli and A. Corigliano are with the Department of Civil and Environmental Engineering of Politecnico di Milano, Milano, Italy (e-mail: valentina.zega@polimi.it, luca4.martinelli@mail.polimi.it, alberto.corigliano@polimi.it).

R. Casati, E. Zappa, A. Cigada are with the Department of Mechanical Engineering of Politecnico di Milano, Milano, Italy (e-mail: riccardo.casati@polimi.it, emanuele.zappa@polimi.it, alfredo.cigada@polimi.it).

G. Langfelder is with the Department of Electronics, Information and Bioengineering of Politecnico di Milano, Milano, Italy (e-mail: giacomo.langfelder@polimi.it).

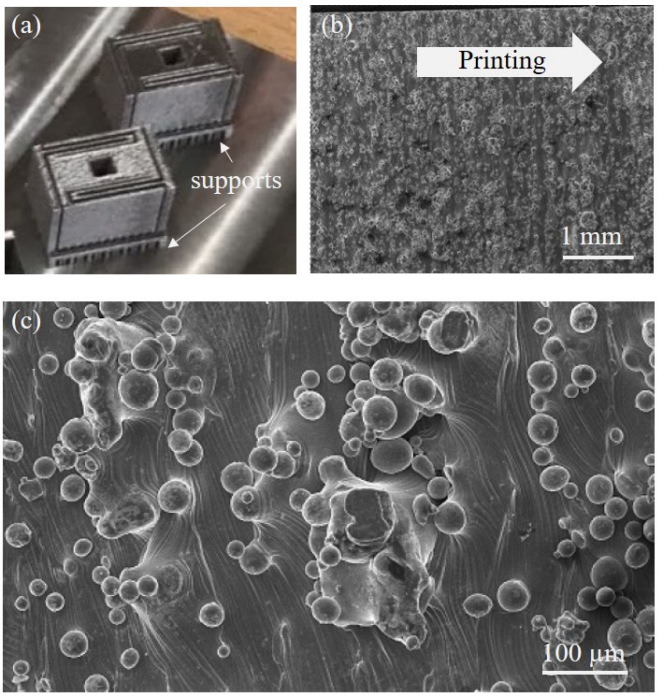

Fig. 2. (a) 3D-printed uniaxial accelerometer. The parts are still welded to the building platform by support structures and electrodes are not glued on the anchor. (b)-(c) SEM image of the surface of the accelerometer's proof mass.

experimental characterization of the first 3D-printed metal capacitive accelerometer. The L-PBF technique is employed to fabricate a Ti6Al4V uniaxial accelerometer with minimum dimensions in the order of hundreds of microns and performances in terms of sensitivity comparable with actual state of the art capacitive MEMS [22]-[23] and 3D-printed sensors [12]-[13].

The paper is organized as follows: Section II describes the mechanical design of the uniaxial accelerometer and the expected performances in terms of sensitivity. Section III introduces the fabrication process and presents a first characterization of the printed prototypes, while in Section IV, the experimental results are reported. Section V closes the paper with conclusions and future perspectives.

II. Mechanical Design of the Uniaxial Accelerometer

The uniaxial accelerometer (Fig. 1) consists in a proof mass suspended through folded springs that allow its pure translation along the *y*-axis, as shown in Fig. 1b. The springs are properly designed to keep the desired mode (Fig. 1b) at a frequency of around 200 Hz and to move away all undesired spurious modes, as that shown as an example in Fig. 1c, thus guaranteeing low cross-axis sensitivity of the sensor. Typical material properties of bulk Ti6Al4V alloy, namely E = 100GPa, υ = 0.33 and ρ = 4500Kg/m^3, are employed in the following models. We chose such rounded values to partially compensate for the expected discrepancies between the printed and bulk material (i.e. E = 113.8GPa, ρ=4430Kg/m^3 [24]).

The overall dimensions of the accelerometer are 28mm x 23mm x 15mm, while the folded springs cross-section is equal to 0.5mm x 15mm, according to the minimum feature size that

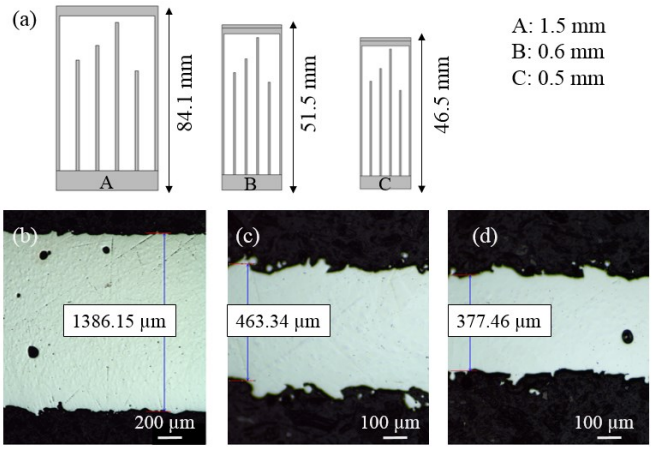

Fig. 3. (a) Schematic view of the three combs of cantilevers. In-plane thickness: 1.5mm (A), 0.6mm (B) and 0.5mm (C). The out-of-plane thickness is equal to 15mm in agreement with the fabricated accelerometer. Optical microscope images of the cantilevers of nominal thicknesses: (b) 1.5mm, (c) 0.6mm and (d) 0.5mm.

can be printed confidently through the L-PBF system used for this research (see Section III for more details).

The external frame (colored in green in Fig. 1a) is shaped to anchor the folded springs and to provide the supports where the electrodes employed for the electrostatic readout are glued. Two PVC sheets are also employed in the assembly procedure to provide electrical isolation between the electrodes and the proof mass of the accelerometer.

At rest, the nominal gap between the accelerometer proof mass and the two electrodes is equal to 300µm, i.e. the total thickness of the PVC sheets employed in the assembly. When an external acceleration is applied along the *y*-axis, the proof mass displaces towards or away from the electrodes according to the first *y*-axis translational mode (Fig. 1b). Being the proof mass and the two electrodes kept at a constant voltage, the displacement of the proof mass causes a differential capacitance variation that allows the external acceleration detection [25]. The expression of the sensitivity for a differential capacitive accelerometer is given by:

$$\frac{\Delta C}{N_g} = 2\frac{C_0}{g_0}\frac{1}{\omega_0^2}9.8\frac{m}{s^2} = \frac{2\epsilon_0 A}{g_0^2}\frac{1}{\omega_0^2}9.8\frac{m}{s^2} \quad (1)$$

where ϵ_0 is the permittivity of air taken as that of vacuum for the sake of simplicity, N_g is the external acceleration expressed in gravity units, A (23mm x 15mm) is the facing electrodes area, ω_0 is the natural frequency, C_0 is the nominal active capacitance at each electrode in absence of any external acceleration and g_0 is the nominal gap between the proof mass and the electrodes. By substituting the geometric dimensions of the device under study, we obtain a theoretical C_0 of 10.2pF and a sensitivity of 421fF/g.

III. Fabrication Process

A L-PBF system was used to print the accelerometers that were manually assembled with Cu electrodes employed for the electrostatic readout.

TABLE I
NATURAL FREQUENCIES OF THE CANTILEVERS OF EACH OF THE THREE FABRICATED COMBS. THEORETICAL ESTIMATION FROM MODAL ANALYSIS, EXPERIMENTAL MEASUREMENTS THROUGH THE HIGH-SPEED CAMERA AND PERCENTAGE ERRORS.

Comb [-]	Theoretical [Hz]	Exp. (Camera) [Hz]	Error (%)
A	250	248.5	0.6
	350	343.1	2.0
	450	435.8	3.2
	550	438.9	20.2
B	250	212.9	14.8
	350	291.7	16.7
	450	332.6	26.1
	550	429.8	21.9
C	250	200.6	19.8
	350	291.7	16.7
	450	375.2	16.6
	550	457.1	16.9

Specifically, the Renishaw AM 250 system was used to manufacture the devices by using a gas atomized Ti6Al4V powder with particle size distribution between 20 and 63µm. The L-PBF system is equipped with a single mode fiber laser with 200W maximum power and estimated beam diameter at focal point of 75µm. The system utilizes pulsed wave emission, which produces discrete and partially overlapped melting spots. The laser power, hatch distance, point distance, and exposure time were set to 200W, 95µm, 65µm, and 70µs, respectively. The specimens were produced under Ar atmosphere using a meander scanning strategy and a layer thickness of 60µm.

The accelerometers were connected to the building platform by means of block-type support structures (Fig. 2a). A belt-saw was employed to cut the supports and remove the parts from the substrate.

It is worth noting that due to the size of the melt pools, parts with thickness smaller than 200-300µm can barely be fabricated. A safe limit of 500µm was considered in this work to guarantee good mechanical properties of the printed sensor.

From the SEM images shown in Fig. 2b-c, it is evident that powder particles welded onto the surface and metal asperities play a crucial role on surface roughness, thus introducing an uncertainty in the nominal gap size between the proof mass and the electrodes.

To further inspect the fabrication tolerances and the final mechanical properties of the printed sensors, three test devices were also fabricated using the same L-PBF system and processing parameters listed above. They consist in combs of cantilevers of different thickness and length, as shown in Fig. 3a. In particular, each comb comprises four cantilevers having the same cross-section and different lengths chosen to let them vibrate at first natural frequencies of 250 Hz, 350 Hz, 450 Hz and 550 Hz. Comb A is characterized by 1.5mm x 15mm cross-section cantilevers of lengths 50.4mm, 57.1mm, 67.6mm and 45.5mm, comb B by 0.6mm x 15mm cross-section beams of lengths 31.8mm, 36.1mm, 42.7mm and 28.8mm, while cantilevers of comb C have a cross-section of 0.5mm x 15mm and lengths 29.1mm, 33mm, 39mm and 26.3mm.

The cross sections of the cantilevers were inspected through an optical microscope and representative pictures are shown in Fig. 3b-d. It is evident that the thickness of the cantilevers differs from the nominal one. Moreover, the discrepancy between nominal and real dimension increases from 8% to about 25% by reducing the cantilever thickness. Indeed, surface defects being of the same dimensions for the three designs, become more significant in terms of stiffness reduction as thickness decreases. Being the thickness of the accelerometers under study nominally equal to 0.5mm, a 25% reduction is expected on the fabricated device.

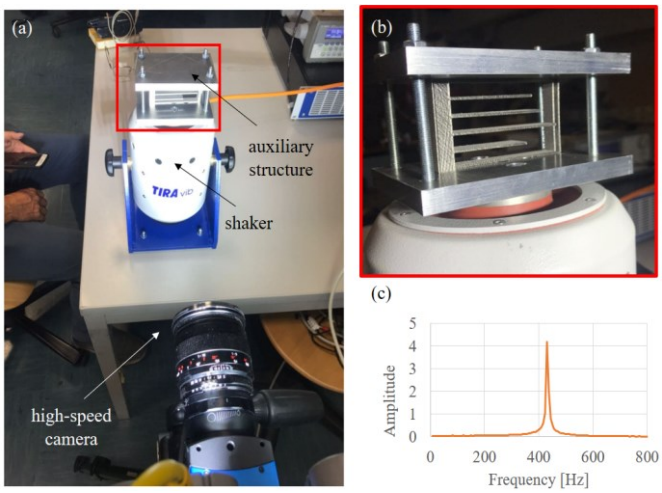

Fig. 4. (a) Experimental set-up for the dynamic characterization of the cantilevers comb. (b) Close-up view of the cantilevers comb mounted on the shaker. (c) Frequency response measured through the high speed camera on the fourth cantilever of comb C.

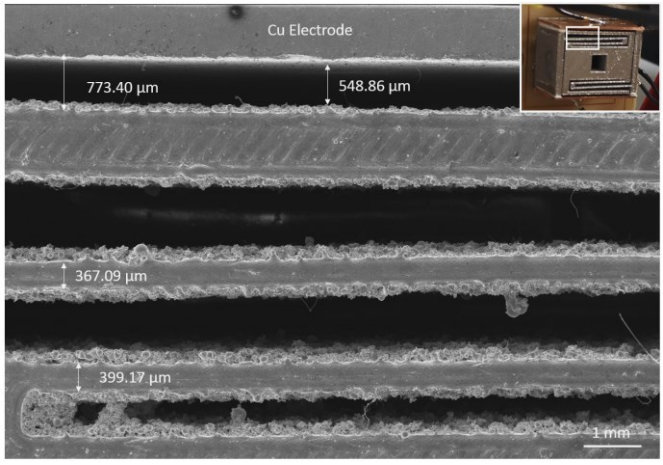

Fig. 5. SEM image of the top-left corner of the uniaxial accelerometer.

Finally, the software ImageJ for image analysis was used to estimate the relative density of the cantilevers from optical micrographs. The L-PBF material shows an average relative density of 99.5%, confirming that the printing parameters were suitable for the production of thin wall objects.

IV. EXPERIMENTAL TESTS

A. *Mechanical Characterization of the cantilevers comb*

The dynamic mechanical characterization of the cantilevers combs fabricated with the same process parameters employed for the accelerometer under study was performed to confirm the

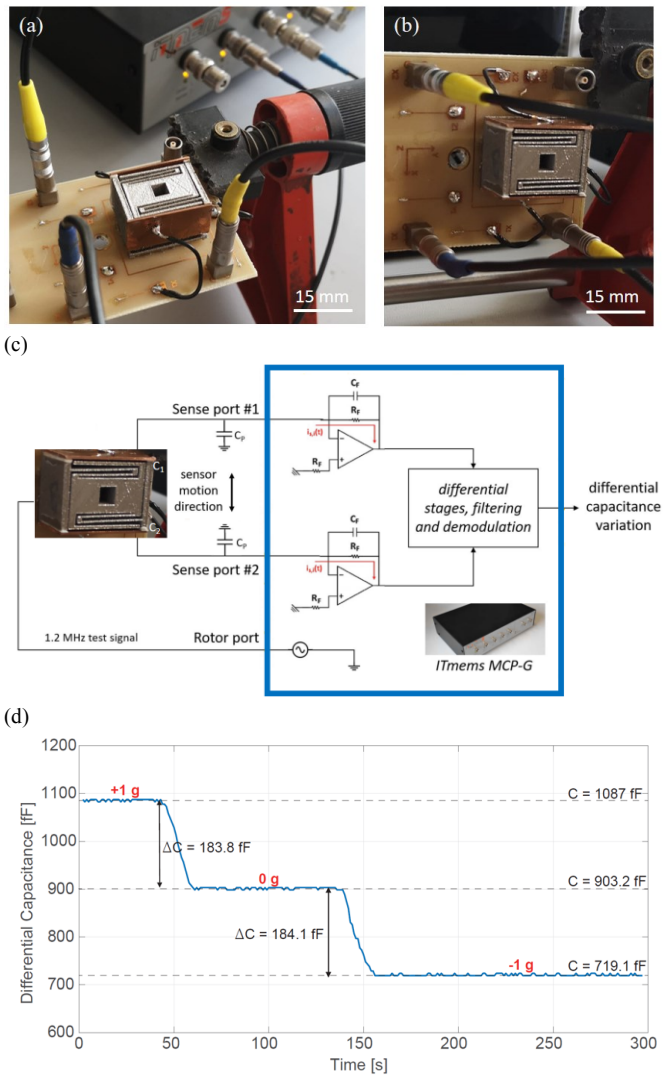

Fig. 6. Experimental set-up. The PCB with the uniaxial accelerometer is mounted in (a) an horizontal direction corresponding to the 0g condition and in (b) a vertical direction to measure the *y*-axis ±1g acceleration. (c) Front-end electronics of the ITMems s.r.l. platform: the sensing electronic chain is put in evidence. The AC test signal applied at the rotor port has a frequency of 1.2MHz and an amplitude of 100 mV_{rms}. (d) Differential capacitance measured by manually applying ±1g in the *y*-axis direction.

reduction of thickness measured through microscope inspection.

Each printed cantilevers comb is mounted on an electromagnetic shaker (Ling Dynamic Systems (LDS) V400 Series) through an auxiliary structure as shown in Fig. 4a-b. For each comb, the natural frequencies of each of the four cantilevers is estimated by applying a sweep excitation around the nominal frequency values and detecting the maximum amplitude condition with a high-speed camera (Mikrotron EoSens mini2) with 100mm focal length ZEISS optics [26]. Then, a stationary harmonic vibration at each detected natural frequency is applied and the dynamic response of the prototype is measured for 50 oscillation cycles. The frame rate of the camera is set to 10240Hz, while exposure time is 98µs. To ensure a proper illumination for the short exposure time, two high power LED lights (Smart Vision Lights SC75-WHI-W 75mm) are employed.

The proposed measuring technique is based on the pattern matching algorithm: a vision-based method that allows recovering the in-plane displacement and orientation of a target, by means of its image acquired by a single camera [27]-[28]. Sub-pixel capability of pattern matching algorithms allows to estimate the pattern displacements with sub-pixel resolution. To recover the pixel-to-millimeter scaling and to compensate for the aberration due to the optics, the camera has been previously calibrated with a 2D state of the art calibration approach [29].

The pattern matching technique allows estimating the motion of a predefined target in each image of the acquired sequence; hence, the full displacement time history can be measured. Thanks to the intense illumination, the exposure time can be set to the mentioned value of 98µs, allowing to neglect the uncertainty due to motion blur [30].

Pattern matching was applied to two portions of the accelerometer, namely the accelerometer frame and the cantilever tip to estimate the displacements provided by the shaker (i.e. input) and the output, respectively. The dynamic response of the system is then reconstructed from this information (Fig. 4c).

Experimental results in terms of natural frequencies are reported in Table I in comparison with those simulated by COMSOL Multiphysics through modal analysis. As already evidenced in the previous Section, an error up to 25% on the in-plane thickness of the cantilevers is possible due to the presence of reduced and inhomogeneous thickness of the cantilever. If we focus on the comb C, we can notice that by considering in the theoretical model an in-plane thickness of 377µm (Fig. 3b) instead of the nominal 500µm we obtain resonant frequencies of 193Hz (-4%), 270Hz (-7.8%), 348Hz (-7.8%) and 426Hz (-7.3%) which are much closer to the experimental values. Similar results can be obtained by taking into account comb B whereby considering in the theoretical model an in-plane thickness of 466µm (Fig. 3c) instead of the nominal 600µm, one obtains resonant frequencies of 197.3Hz (-7.9%), 276.6Hz (-5.5%), 356.9Hz (6.8%) and 435.8Hz (1.4%).

Thus, dynamic measurements confirm the fabrication tolerances put in evidence in the previous section and prove the validity of the actual numerical model to predict, with an error smaller than 8%, the resonant frequencies of deformable components 3D-printed by LPBF.

Unfortunately, it is not possible to reduce the error for the variability of the surface roughness which is related to the size of powder particle sticked onto the surface. Only a visual inspection of all the components can indeed guarantee an exact estimation of the part geometry.

B. Mechanical Characterization of the uniaxial accelerometer

Once the fabrication process properties are investigated, a first mechanical characterization of the accelerometer is performed with the purpose to detect its resonant frequency.

The printed prototype is mounted on an electromagnetic shaker (Ling Dynamic Systems (LDS) V400 Series) through an auxiliary structure to be excited with a pure sinusoidal signal.

The dynamic response of the accelerometer is measured through the same technique described in Section IVA. In this

case, the frame rate is set to 5120Hz, while exposure time is 150µs. Pattern Matching technique is applied to the acquired image sequences two times: first to track the motion of the auxiliary structure (input signal) and then to estimate the motion of the suspended mass (output). The transfer function is then computed with a step sine approach, allowing to estimate the resonance frequency of the two prototypes as the peak of the experimental transfer function. The experimental natural frequencies are 155Hz and 158.5Hz: compatible with the 25% thickness reduction of the folded springs predicted through the analyses on the cantilevers comb and with the direct measurement of the geometric dimensions through SEM (Fig. 5). Moreover, the fact that the natural frequency of the two prototypes is almost the same, can be taken as proof of consistency of the behavior.

C. *Electrical Measurements*

The 3D-printed uniaxial accelerometer is finally assembled with the Cu electrodes as shown in Fig. 6a. Two PVC sheets of total thickness 300µm are employed to provide electrical insulation and to define a gap between the accelerometer proof mass and the electrodes. Note that the manual assembly of the accelerometer with the Cu electrodes introduces uncertainties on the real gap between the mass and the electrodes, which is reasonably expected to be bigger than the nominal 300µm.

The assembled sensor is then glued to a printed circuit board (PCB) and the three electrical contacts, i.e. the proof mass and the two electrodes, are soldered at low temperature to pads which are in turn routed to electrical connectors (Fig. 6a). No package is considered in the experimental campaign.

At first, the PCB is mounted in the horizontal direction, i.e. 0g condition, and the initial capacitances between the electrodes and the proof mass are measured to check asymmetries due to fabrication imperfections, e.g. residual stresses and surface roughness, and the manual assembly. The MEMS characterization platform (MCP) from *ITmems srl*, a tool specifically developed for testing of capacitive accelerometers and gyroscopes [31]-[32] is employed for this purpose. In Fig. 6c the front-end electronics implemented in the commercial platform is shown and the sensing electronic chain is highlighted. A capacitance of 8.6pF is measured between the proof mass and the first electrode, while a capacitance of 9.5pF is measured between the proof mass and the second electrode. A differential offset of 900fF is then obtained. From the measured capacitances, it is possible to estimate the initial gaps between the two electrodes and the proof mass that read 355µm and 321µm, respectively. Note that unknown parasitic capacitances induced by the electric connections play a significant role in the value of the active capacitances measured between the mass and the electrodes and should be taken into account in the gap estimation. As a consequence, we would expect an effective gap larger than the one estimated above by neglecting parasitic capacitances.

A sensitivity measurement is then performed by manually applying ±1g to the accelerometer. The PCB is rotated as shown in Fig. 6b and the differential capacitance between the two electrodes is measured (Fig. 6d). A sensitivity of 184fF/g is obtained which is far less then theoretical estimation. To explain such difference, we analyzed the different sources of error one at a time. At first, fabrication process imperfections on the geometry, i.e. springs and mass, of the accelerometer are neglected and the theoretical value of the natural frequency, i.e. 200 Hz, is considered. From eq. (1) we then estimated a gap between the mass and the electrodes of 453.8µm, much larger than the one estimated through the C_0 measurements by neglecting parasitic capacitances. However, by considering a realistic parasitic capacitance of 2.75pF, the experimental results coincide with theoretical predictions. At second, we considered also the fabrication process imperfections on the geometry of the accelerometer. We then substituted in eq. (1) the experimental natural frequency measured in Section IVB, i.e. 158.5Hz, and we got a gap between the mass and the electrodes of 572.5µm which is bigger than the one estimated before. However, also in this case, a good agreement with theoretical predictions can be achieved by considering a parasitic capacitance of 4.2pF which is as well reasonable for the employed setup. To validate our hypotheses on the gap between the Cu electrodes and the uniaxial accelerometer, we made a direct measurement of it through a SEM (Fig. 5). A satisfactory agreement is then achieved between experiments and theoretical predictions. Moreover, from Fig.6d it is evident a linear behavior of the accelerometer in the considered range of frequency.

For comparison, typical differential sensitivities of state-of-the-art MEMS accelerometers are near to 5fF/g [22], which is about a factor 20 less than the measured results. In Tab.II we report a comparison between different capacitive accelerometers fabricated both through MEMS standard processes and 3D-printing techniques. It is clear that the proposed device is strongly competitive with actual state of the art and can reach outstanding performances once the process is optimized. Moreover, the large sensitivity, coupled to the large proof mass, indicates that electronic noise of an electronic readout chain analogous to those already employed for MEMS-based solutions could be made negligible, providing a solution for ultra-low noise systems.

TABLE II
COMPARISON BETWEEN MEMS AND 3D-PRINTED CAPACITIVE ACCELEROMETERS WITH THE PRESENT WORK IN TERMS OF DIMENSIONS AND SENSITIVITY.

	Sensitivity	Dimensions
[22]	5 fF/g	0.4 x 0.6 x 0.1 mm^3
[23]	8.7 pF/g	4 x 4 x 0.59 mm^3
[12]	33.16 fF/g	30.4 x 9 x 2 mm^3
[12]	31.44 fF/g	22.4 x 9 x 2 mm^3
[this work]	184 fF/g	28 x 23 x 15 mm^3

V. CONCLUSIONS

In this work, the first uniaxial 3D-printed metal accelerometer is designed, fabricated and tested. It shows good performances in terms of sensitivity and represents a promising solution for ultra-low noise, cheap and customizable systems. Moreover, the proposed Ti6Al4V uniaxial accelerometer can in principle overcome the main limitations of polymer based 3D-printed sensors in terms of operation in harsh environments, e.g. high temperature. Ti6Al4V shows indeed a specific heat of

553J/Kg K, a thermal conductivity of 6.6-6.8W/m K and a thermal expansion coefficient of $8.6 \cdot 10^{-6} K^{-1}$ [24], that guarantee a much better thermal behavior than polymer based sensors, whose thermal expansion coefficients are usually at least one order of magnitude bigger [33]-[34] and that can only operate far below the glass-transition temperature [35]. A different consideration must be done if we want to compare metal sensors as the one here proposed, with polymer based sensors metallized through a Cu layer [12]-[14]. In this case, as already put in evidence in [12], the thermal behavior is dominated by the Cu layer (thermal expansion coefficient = $17 \cdot 10^{-6} K^{-1}$, thermal conductivity = 3.94W/m K, specific heat = 385J/ Kg K), but so far there are no experimental evidence of the right functioning of the sensor above the glass-transition temperature of the inner polymeric mechanical structure. The proposed Ti6Al4V uniaxial accelerometer indeed seems a very promising solution for harsh environments if compared with actual state of the art 3D-printed sensors.

The L-PBF technique is here employed for the fabrication of the proposed accelerometer and fabrication imperfections are studied in details through test structures. Both visual and electrostatic measurements prove the right functioning of the accelerometer and emphasize the versatility of the proposed sensor. Despite the dimensions of the proposed accelerometer are not comparable with the ones of MEMS, this work opens the path to a new class of 3D-printed metal sensors that are easy to fabricate and personalize.

We are currently working to improve the fabrication process, i.e. imperfections reduction, and the experimental set-up, i.e. parasitic capacitance reduction, to achieve a smaller discrepancy between theoretical values and experiments. Further measurements will be also performed to test the performances of the proposed device in harsh environments and to prove the linearity of its response up to elevated accelerations.

REFERENCES

[1] A. Corigliano, R. Ardito, C. Comi, A. Frangi, A. Ghisi and S. Mariani (2018). Mechanics of Microsystems, *Wiley*, ISBN 978-1-119-05383-5.

[2] Ph. Robert, V. Nguyen, S. Hentz, L. Duraffourg, G. Jourdan, J. Arcamone and S. Harrisson, "M&NEMS: A new approach for ultra-low cost 3D inertial sensors", in *IEEE Sensors*, Christchurch, 2009, pp. 963-966.

[3] Y. Xu, X. Wu, X. Guo, B. Kong, M. Zhang, X. Qian, S. Mi and W. Sun. "The boom in 3D-printed sensor technology", *Sensors*, vol. 17, pp. 1166, 2007.

[4] T. D. Ngo, A. Kashani, G. Imbalzano, K. T.Q. Nguyen, D. Hui. "Additive manufacturing (3D printing): A review of materials, methods, applications and challenges", *Composites Part B: Eng*., vol. 143, pp. 172-196, 2018.

[5] M. R. Khosravani, T. Reinicke "3D-printed sensors: current progress and future challenges", *Sensors and Actuators A: physical*, vol. 305, pp. 111916, 2020.

[6] T. Han, S. Kundu, A. Nag and Y. Xu "3D Printed sensors for biomedical applications: a review", *MDPI Sensors*, vol.19, n. 7, pp. 1706, 2019.

[7] D. Espalin, D. W. Muse, E. MacDonald, R. B. Wicker "3D Printing multifunctionality: structures with electronics", *Int. J. Adv. Manuf. Technol.*, vol. 72, pp. 963-978, 2014.

[8] H. Yang, W. R. Leow, X. Chen "3D Printing of flexible electronic devices", *Small Methods,* vol. 2, pp. 1700259, 2017.

[9] L.-M. Faller, M. Krivec, A. Abram, H. Zangl AM "Metal Substrates for Inkjet-Printing of Smart Devices", *Materials Characteriz*., vol. 143, pp. 211-220, 2018.

[10] L.-M. Faller, M. Lenzhofer, C. Hirschl, M. Kraft and H. Zangl "Characterization of a robust 3D- and Inkjet-Printed capacitive position sensor for a spectrometer application", *Sensors*, vol. 19, n. 3, pp. 443, 2019.

[11] Y. Sui and C. A. Zorman "Review- Inkjet printing of metal structures for electrochemical sensor applications", *J. Electrochemical Society*, vol. 167, pp. 037571, 2020.

[12] V. Zega, C. Credi, R. Bernasconi, G. Langfelder, L. Magagnin, M. Levi and A. Corigliano "The first 3D-printed z-axis accelerometers with differential capacitive sensing", *IEEE sensors journal,* vol. 18, n. 1, pp. 53-60, 2018.

[13] V. Zega, M. Invernizzi, R. Bernasconi, F. Cuneo, G. Langfelder, L. Magagnin, M. Levi and A. Corigliano "The first 3D-Printed and wet-metallized three-axis accelerometer with differential capacitive sensing", *IEEE sensors journal,* vol. 19, n. 20, pp. 9131-9138, 2019.

[14] L. Gaffuri Pagani, P. Carulli, V. Zega, R. Suriano, R. Bernasconi, A. Frangi, M. Levi, L. Magagnin, G. Langfelder "The first three-dimensional printed and wet-metallized Coriolis mass flowmeter", *IEEE sensors letters*, vol. 4, n. 6, pp. 9096411, 2020.

[15] E.O. Olakanmi, R.F. Cochrane, K.W. Dalgarno "A review on selective laser sintering/melting (SLS/SLM) of aluminium alloy powders: processing, microstricture, and properties", *Progress in Materials Science*, vol. 74, pp. 401-477, 2015.

[16] D. Agius, K.I. Kourousis and C. Wallbrink "A review of the as-built SLM Ti-6Al-4V Mechanical properties towards achieving fatigue resistant designs", *Metals*, vol. 8, n. 1, pp. 75, 2018.

[17] K. Karolewska and B. Ligaj "Comparison analysis of titanium alloy Ti6Al4V produced by metallurgical and 3D printing method", *AIP Conf. Proceed.* 2077, 020025, 2019.

[18] B. Wysocki, P. Maj, A.T. Krawczynska, J. Zdunek, K. Rozniatowski, K.J. Kurzydlowski, W. Swieszkowski "Microstructure and mechanical properties investigation of CP titanium processed by selective laser melting (SLM)", vol. 241, pp. 13-23, 2016.

[19] T. DebRoy, H.L. Wei, J.S. Zuback, T. Mukherjee, J.W. Elmer, J.O. Milewski, A.M. Beese, A. Wilson-Heid, A. De, W. Zhang "Additive manufacturing of metallic components – Process, structure and properties", *Progress in Materials Science,* vol. 92, pp. 112–224, 2018.

[20] P. Stoll, B. Leutenecker, A.B. Spierings, C. Klahn, K. Wegener "Temperature monitoring of an SLM part with embedded sensor", *Int. Conf. on Additive Manufactoring in Products and Applications*, Sept. 2018.

[21] T.G. Spears, S.A. Gold "In-process sensing in selective laser melting (SLM) additive manufacturing", *Integrating Materials and Manufactoring Innovation*, vol. 5, pp. 16-40, 2016.

[22] F. Maspero, S. Delachanal, A. Berthelot, L. Joet, G. Langfelder and S. Hentz, "Quarter-mm2 High Dynamic Range Silicon Capacitive Accelerometer with a 3D Process" *IEEE Sensors Journal*, vol. 20, no. 2, pp. 689-699, 2020.

[23] X. Zhou, L. Che, J. Wu, X. Li, Y. Wang, "A novel sandwich capacitive accelerometer with a symmetrical structure fabricated from a D-SOI wafer", J. Micromech. Microeng., vol. 22, pp. 085031, 2012.

[24] ASM Handbook Volume 2: Properties and Selection: Nonferrous Alloys and Special Purpose Materials, *ASM International*, ISBN: 978-0-87170-378-1, 1990.

[25] G. Langfelder and A. Tocchio. "Differential Fringe- Field MEMS Accelerometer", *IEEE Transactions on Electronic Devices*, vol. 59, n. 2, pp. 485-490, 2012.

[26] A. Bonanomi, E. Zappa, A. Cigada, V. Zega, A. Corigliano. "High speed vision system for the dynamic characterization of 3D printed sensors", *IOP Conf. Series: J. Physics*, vol. *1249*, 012001, 2019.

[27] G.M. Landau, U. Vishkin, "Pattern matching in a digitized image". *Algorithmica*, vol. 12, pp. 375–408, 1994.

[28] R. Brunelli, "Template Matching Techniques in Computer Vision: Theory and Practice", March 2009, ISBN: 978-0-470-51706-2.

[29] G. D'Emilia, D. Di Gasbarro, "Review of techniques for 2D camera calibration suitable for industrial vision systems", *Journal of Physics: Conference Series*, vol. 841, 7th Young Researcher Meeting 24–26 October 2016, Torino, Italy.

[30] A. Lavatelli, E. Zappa, "A Displacement Uncertainty Model for 2-D DIC Measurement Under Motion Blur Conditions", *IEEE Transactions on Instrumentation and Measurement*, vol. 66, no. 3, 2017.

[31] C. Buffa, A. Tocchio and G. Langfelder "A Versatile Instrument for the Characterization of Capacitive Micro- and Nanoelectromechanical Systems", *IEEE Transactions on Instrumentation and Measurement*, vol. 61 n. 7, pp. 2012-2021, 2012.

[32] http://www.itmems.it/?news=09222016-itmems-mcp-handbook

[33] C. Wang, V. I. Kondrashchenko, A.V. Matseevich, "Prediction of the coefficient of thermal expansion of building materials based on polyvinyl chloride" *J. Phys. Conf. Ser*., vol. 1425, p. 012094, 2019.

[34] V. Arumugam, C. R. Kumar, G.M. Joshi, "Polymer composites for thermal management: a review" *Composite Interfaces*, vol. 23, no. 9, pp. 1-26, 2016.
[35] Polymer Properties Database. Access on 15/04/2021. Website: http://polymerdatabase.com/polymer%20physics/Polymer%20Tg%20C.html

Valentina Zega received the Ph.D. degree in structural, seismic, and geotechnical engineering from Politecnico di Milano in 2017. She is currently an Assistant Professor with the Department of Civil and Environmental Engineering, Politecnico di Milano. She has co-authored around 40 papers and three deposited patents. Since 2019, she has been a TPC member in the *IEEE MEMS* and *IEEE EFTF-IFCS* conferences. Her research interests include the mechanical design and optimization of MEMS devices and metamaterials and the numerical modeling of their linear and nonlinear dynamic response.

Luca Martinelli received the B.Sc in Materials Engineering and Nanotechnology and the Double M.Sc. degree, both in Materials Engineering and Mechanical Engineering in 2020 from Politecnico di Milano. During the bachelor thesis, he studied nanostructured titanium oxide films for photocatalitic applications, while the master thesis was focused on 3D-Printed Titanium Accelerometers. He is passionate about science and technology, with particular focus on the Additive Manufacturing field.

Riccardo Casati is Associate Professor of metallurgy at the Department of Mechanical Engineering of the Politecnico di Milano. His research deals with the evolution of microstructure and mechanical behavior of metallic materials during manufacturing and service. In recent years, his scientific activity has focused on alloys and composites produced by powder metallurgy and additive manufacturing processes. He is co-author of more than hundred papers published in scientific journals and conference proceedings.

Emanuele Zappa is Full Professor in Mechanical and Thermal Measurements at Politecnico di Milano, Italy. He is Associate Editor of the IEEE Transaction on Instrumentation and Measurement. The scientific activity is mainly in the field of mechanical and image-based measurements, focusing on the measuring techniques development, the applications in complex and hostile environments, as well as the qualification and reduction of the measuring uncertainty in dynamic applications.

Giacomo Langfelder received the Ph.D. degree in Information Technology in 2009 from Politecnico di Milano, Italy, where he is now an Associate Professor of MEMS and microsensors.
His research focuses on CMOS sensors, MEMS, and related electronics. He is the author of about 100 refereed publications and holds 7 patents. Since 2017, he has been an associate editor for the *IEEE Sensors Letters*. Since 2016, he has been a TPC member in the *IEEE MEMS* and in the *IEEE Inertial Sensors* conferences. In 2014, he was a co-founder of ITmems s.r.l. Dr. Langfelder was the recipient of the Premio di Laurea Accenture in 2005 and the Premio per la Promozione della Ricerca Scientifica in 2011, granted by Rotary International.

Alfredo Cigada (b.1965, M.Sc. Mechanical Engineering, PhD Mechanical Engineering) is Professor of Mechanical Measurements at Politecnico di Milano. His main research topics are in the field of new measurement systems, with a focus on MEMS and fiber optic sensors, and on data management. The main applications are in the area of Structural Health Monitoring for civil structures and cultural heritage.

Alberto Corigliano is full professor of Solids and Structural Mechanics with the Department of Civil and Environmental Eng. of Politecnico di Milano. He is member of the technical committee of Eurosime, Associate Editor of the European Journal of Mechanics A/Solids, of Advanced Modelling and Simulation in Eng. Sciences and of Frontiers in Materials – Mechanics of materials. In 2006 he won the Bruno Finzi prize for Rational Mechanics given by the "Istituto Lombardo Accademia di Scienze e Lettere", in July 2015 he was appointed Euromech Fellow by the European Mechanics Society. In 2018 he was elected member of the "Istituto Lombardo Academia di Scienze e Lettere". He is (co-) author of more than 280 papers, published on international (more than 110) and Italian technical journals, and 11 patents or filed patents. His present research interests include: MEMS modelling and design, additive manufacturing for sensors, metamaterials, deep learning combined with physical modelling for materials and structural monitoring.